Physica B: Condensed Matter 551 (2018) 191–196

Contents lists available at ScienceDirect

Physica B: Condensed Matter

journal homepage: www.elsevier.com/locate/physb

Effects of doxorubicin on the structural and morphological characterization of solid lipid nanoparticles (SLN) using small angle neutron scattering (SANS) and small angle X-ray scattering (SAXS)

Fabiano Yokaichiya [a,*], Christian Schmidt [b], Joachim Storsberg [b], Mont Kumpugdee Vollrath [c], Daniele Ribeiro de Araujo [d], Ben Kent [a], Daniel Clemens [a], Friedrich Wingert [b], Margareth K.K.D. Franco [e]

[a] Helmholtz-Zentrum-Berlin, Germany
[b] Fraunhofer Institute Applied Polymer Research (IAP), Germany
[c] Beuth Hochschule für Technik Berlin (BeuthHS), Germany
[d] Universidade Federal do ABC, Brazil
[e] Instituto de Pesquisas Energéticas e Nucleares–IPEN, Brazil

ARTICLE INFO

Keywords:
Doxorubicin
SANS
SLN
Soybean
Mygliol

ABSTRACT

Cancer is still a major public health problem. Leaving detection of early stages of tumors and other issues aside, minimizing unwarranted side effects, for example after clinical usage of a liposomal anticancer drug doxorubicin (Dox) formulation, is an unmet clinical problem and the focus of many studies. Using compounds typically used in the preparation of food and/or cosmetics to prepare drug carrier systems, we observed that sodium tetradecyl sulfate (STS) containing and soybean-oil based carriers are more efficient in reducing the viability of HeLa cells tumor cells in comparison to their respective counterparts. Here, we probe the doxorubicin (Dox) loading on structural properties of either soybean oil or coconut oil (Mygliol 812) formulations. Small angle neutron scattering (SANS) assays were performed using V16 instrument at Helmholtz-Zentrum Berlin (HZB) at 25, 37 and 40 °C with two or 11 m distance between detector and sample to assess a wide range in scattering vector Q. Combined with previous measurement using small angle X-ray scattering (SAXS), our results show that the Dox has different influence in the surface structure of the solid lipid nanoparticles (SLN) and also affects the fractality in the vesicle aggregates when the concentration of the drug is altered, for Mygliol and soybean oil SLN drug delivery carrier systems.

1. Introduction

Cancer is a major public health problem worldwide. In United States, cancerous lesions is the second leading cause of death [1,2]. Advances in the clinical management of cancer consist of applications of pharmacologically active substances which achieve the cytotoxicity impact upon tumorigenic cells, however, these are frequently accompanied by undesired adverse effects [3,4]. In the interest of reducing the unforeseen chemotherapy-associated toxicity profile for cancer patients, further research in the development of new therapeutic formulations is essential. Consequently, the development of targeted drug delivery systems with a long shelf life, optimal drug loading profile and low inherent toxicity is an important approach to address this unmet clinical need [5,6].

Doxorubicin (Dox) is one of the most potent chemotherapeutic drugs [7,8] applied to cancer treatment, including breast, lung, gastric, ovarian, thyroid, non-Hodgkin's and Hodgkin's lymphoma, multiple myeloma, sarcoma and pediatric cancers [9]. Dox can be applied either alone [10–12] or combined with other treatment options [13], Dox efficacy is widely acknowledged due to its ability to combat rapidly dividing cells and slow the disease progression. On the other hand, its toxicity to noncancerous cells in the human body is a limiting point in its medical application. Dox-induced toxicity affects organs such as the liver, kidneys, and brain, but has the most effect on the heart (cardiotoxicity). Recent studies reported that Dox can cause structural alterations in the

* Corresponding author. Institut Quantenphänomene in neuen Materialien (EM-IQM), Helmholtz-Zentrum Berlin für Materialien und Energie GmbH, Hahn-Meitner-Platz 1, D-141 09, Berlin, Germany.
E-mail address: fabiano.yokaichiya@helmholtz-berlin.de (F. Yokaichiya).

https://doi.org/10.1016/j.physb.2017.12.036
Received 31 August 2017; Received in revised form 10 December 2017; Accepted 14 December 2017
Available online 14 December 2017
0921-4526/

cardiomyocytes in the heart [8] and also can induce mitochondrial accumulation of iron and pursuant to cardiomyopathy [14].

Dox belongs to a non selective class I an thracycline [15] in which its chemical composition possesses two main parts: aglyconic and sugar moieties. In the aglyconic moiety, Dox has a tetracyclic ring with quinine-hydroquinone adjacent groups, methoxy substituent short side chain followed by a carbonyl group. In the sugar part, known as daumosamine, there is a glycosidic bound attached to one of the rings. This is included of a 3-amino-2,3,4-trideoxy-L-fucosyl component [16].

Due to advances in the study of drug delivery carriers, it can be observed in the literature [17] that the cardiac toxicity of liposomal formulated Doxis was less than that of conventional Dox, while its efficacy remained comparable. Accordingly, on February 4th, 2013, the lack of the brand Doxil in the US market, urged the U. S. Food and Drug Administration to accept the usage of a generic version of this liposomal Dox formulation for cancer treatment [18]. Although the cardiotoxicity related to the liposomal Dox formulation was less than that of conventional Dox, there is a probable correlation between the liposomal formulation used in the clinical setting and occurrence of hand-and-foot-syndrome (HFS) [19,20].

Lipid-based colloidal carriers used for the administration of lipophilic drugs and reduction of local toxicity are widely known and have been investigated for many years. The possibility of modulating drug release in order to facilitate the drug transport to different biological tissues (like tumor, inflammatory cells, a large variety of organs (liver, lung, heart)) is a key characteristic of these carriers systems. Furthermore, they increase the local penetration, extend residence time, and provide a controlled release mechanism in order to supply an effective dose to the target region [21].

Solid lipid nanoparticles (also known by SLN) were introduced in the 1990's as alternative carrier systems to the traditional colloidal phospholipid vesicles and oil-in-water (O/W) emulsions. These systems combine the advantage of the traditional systems while also allowing the possibility of large scale production in a simple cost-effective way [22]. In a previous paper [23], these systems were extensively studied using hydrodynamic particle size, zeta potential and in vitro tests combined with small angle X-ray scattering measurements in order to establish a correlation between the efficacy of the drug delivery system and its surface characteristics. However, it was observed that the complementary analysis given by small angle neutron scattering (SANS), SANS is sensitive to surface characteristics over a large q range and important to get a whole vision of the structure characterization of this solid lipid nanoparticles (SLN). Therefore, the aimed of this study is to correlate the SANS with SAXS data in order to understand the differences between the two target lipid systems, soybean oil and Mygliol 812, used to encapsulate the Dox at a different concentrations of the drug.

2. Materials and methods

2.1. Sample preparation

In order to prepare the samples the following reagents were obtained: 2,6-di-tert-butyl-4-methylphenol (BHT, ACROS, Geel, Belgium), soybean oil (Roth, Karlsruhe, Germany), cetylpalmitate (Roth), sodium tetradecylsulfate (Aldrich, Munich, Germany), Mygliol 812 (Caesar & Loretz, Germany), polysorbate 80 (Roth), 1,2-dimyristoyl-sn-glycero-3-phosphocholine (L-alfa-lecithin, Roth) and doxorubicin (Molecula, Munich, Germany, and Sigma, Munich, Germany). In the Tables 1 and 2 we present the composition of soybean oil and Mygliol 812 employ in this study respectively. It is interesting to observe that in the composition of soybean oil, 86% are unsaturated fatty acids whereas in Mygliol 812, 99% are composed of saturated fatty acids. We followed for the carrier preparation the procedure published by Chinsriwogkul et al. [24] with the following modifications: the aqueous phase consisted of 15.2 g of deuterated water for the samples measured by SANS and light water for samples measured at SAXS instrument, respectively. 1,84 mM [Dox] for loading and 2 g polysorbate 80, whereas the lipid phase, consisted of 300 mg lecithin, 500 mg BHT, 3,75 g cetylpalmitate, and either 3,75 g of soybean oil or Mygliol 812. Both mixtures were preheated to 70 °C under constant agitation using 600 rpm while the aqueous phase was added dropwise to the systems. In a subsequent step, the preparation was sonicated, with the agitation of the mixture continuing at 70 °C for 5 min. Finally the heat source was removed with continual agitation until the mixture reached room temperature (~25 °C). Following the preparation process, five individual sonication steps of 5 min each with a break of 10 s between each step. The setup used in this part of the process is 40% amplitude on a Sonoplus Mini 20 from Bradt Electronics. Once the desired pH of 8 ± 0.1 was achieved, the mixture was passed through 1 μm and 0.45 μm membrane filters successively, then sodium tetradecyl sulfate (STS) was added at a molar ratio of 1.25 mol STS per 1 mol Dox. Finally, the mixture was refrigerated for 3 days and subjected to a final sonication step (3 min; 40% amplitude on Sonoplus Mini 20 from Bradt Electronics).

Table 1
Composition of soybean oil.

Fatty Acids composition for soybean oil	[%]
C 16:0 Palmitic acid	10.62
C 18:0 Stearic acid	2.81
C 18:1 Oleic acid	25.25
C 18:2 Linoleic acid	53.29
C 18:3 Linoleic acid	5.95
C 20:0 Arachidic acid	0.35
C 22:0 Behecid acid	0.70
Trans-isomer fatty acids	1.08

Table 2
Composition of mygliol.

Fatty Acids Composition for Mygliol	[%]
Caproic acid	0.1
Caprylic acid	56.3
Capric acid	43.1
Lauric acid	0.3
Myristic acid	0.1

2.2. Small angle neutron scattering (SANS)

The SANS measurement was performed on the V16 instrument at Helmholtz-Zentrum Berlin (HZB) [25]. The data was recorded at two sample-detector distances: 1.7 m with neutron wavelength 1.8–3.8 Å and 11 m with neutron wavelength 1.6–9.2 Å. Eight samples (soybean oil mixture(S) with Dox concentration S0, S1, S2, S3; and Mygliol 812 mixture (M) with different Dox concentration (M0, M1, M2, M3) were measured at 25, 37 and 40 °C. In order to ensure samples were equilibrated at the measurement temperature, a waiting time of at least 30 min was used. The final data was corrected for sample transmission, background detector counts, empty cell scattering and detector efficiency, and then scaled to absolute intensity using a 1 mm H_2O standard measurement. The data show in this study was radially averaged and combined to give a total q range of: 0.005–0.5 $Å^{-1}$.

2.3. Small angle X-Ray scattering (SAXS)

SAXS measurements were performed at room temperature (25 °C) at the Brazilian Synchrotron Light Laboratory (LNLS) using the SAXS2 beamline with an energy of 8 keV ($\lambda = 1.5498$ Å), wave vector number ranging from 0.25 nm^{-1} to 6.5 nm^{-1}, 1 m distance between sample and the MarCCD detector (diameter of 165 mm) and a customized sample holder [26–28]. Samples were placed into a 600 μm diameter channel to obtain a sample thickness of 1 mm between replace able mica windows [26]. Usage of this device ensured a constant position of the sample in

reference to the beam path. By measuring a buffer solution sample or water sample, which has a scattering curve that is a constant line, we can monitor the background scattering and subtract this intensity curve from the actual sample. Samples were retrieved after data acquisition and the cell was rinsed and dried using nitrogen gas. The background-corrected and normalized scattering intensity was recorded by a 2-dimensional detector (MAR-Rayonix, 165 mm diameter). In the case of isotropic scattering, the beam was set to target the center of the detector. Integration of the area over the solid angle was then used to determine the dependency of the isotropic intensity as a function of the scattering angle.

3. Results and discussion

In a previous study [23], in vitro performance assays using plain carriers (denoted here by S0 and M0) and Dox-loaded carriers (M1 180 μM and S1: 360 μM; M2 and S2:540 μM; M3 and S3: 900 μM) provide potent effects of STS-containing and Dox-loaded soybean (S) oil based solid lipid nanoparticle systems when compared to their respective Mygliol 812 (M) counterpart. Observing this effect, the intention is to obtain structural insights into these carrier systems and correlate them with the in vitro performance results.

For this reason, small angle scattering techniques were applied to get information about the structures of the solid lipid nanoparticles and their aggregates. An overview of the results is displayed in the Fig. 1 for (a) soybean oil SLN and (b) Mygliol 812 SLN. It is possible to observe in the SAXS data peaks related to the cubic structure [33] of the SLN system, q_{c_S1}, q_{c_S2}, q_{c_M1} and q_{c_M2} as displayed in Fig. 1. The obtained values of

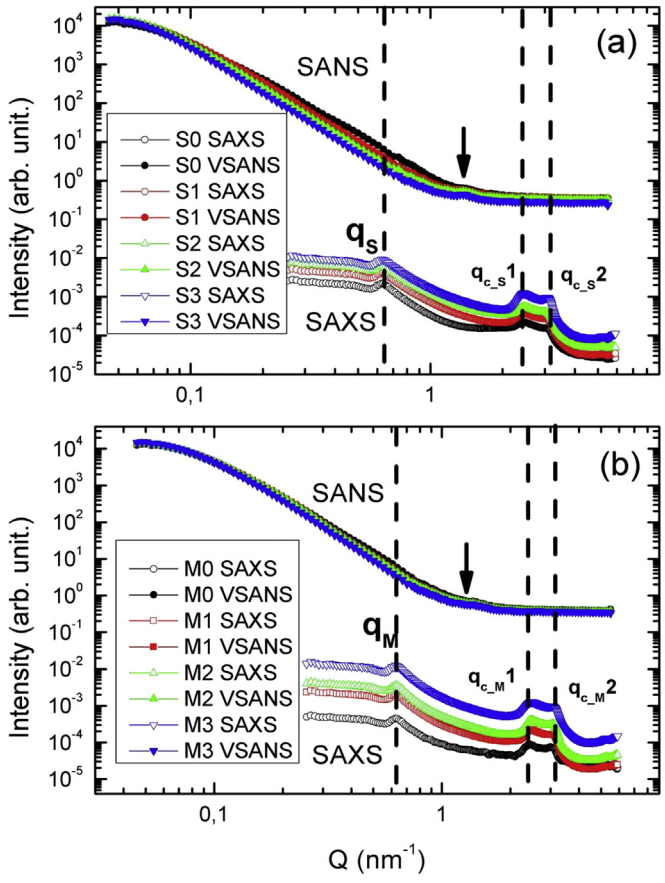

Fig. 1. SANS and SAXS data overview measure at room temperature (25C) for (a) soybean oil (S) SLN and (b) Mygliol 812 (M) SLN. Observe that the peaks from the cubic structure (q_{c_S1}, q_{c_S2}, q_{c_M1} and q_{c_M2}) are only observed at SAXS data. The extra peaks measured at SAXS experiment is probably related to a unusual orthorrombic structure, $q_S = q_M = 0{,}628\ nm^{-1}$. The arrows displayed in both graphics, in VSANS data, can be concerned to the lamellae thickness of the nanoparticles.

$q_{c\_S1} = q_{c\_M1} = 2.5\ nm^{-1}$ and $q_{c\_S2} = q_{c\_M2} = 3{,}02\ nm^{-1}$ are reported in the reference [23]. Depending on the q range, indication of the fractality at submicrometer and nanometers scales can be conveniently obtained from the small angle scattering intensity $I(q)$ on established dimensional analysis. In the q range measured with SAXS technique, using the power law of scattering intensity, described as $I(q) \sim q^{-\alpha}$, information of the surface roughness was achieved (Porod's law) for all the systems [23,31]. The results show [23] that for blank carriers (S0 and M0) the $|\alpha|$ parameter is 4, indicating a smooth surface for the nanoparticles. On the other hand, when the Dox is added to the systems, different effects were observed on the fractality of the surface of the nanoparticle. For soybean oil systems, the $|\alpha|$ parameter was lower than 4 (3.7 for S1, 3.6 for S2 and 3.5 for S3) implying a rough surface [23]. For Mygliol nanoparticles, the $|\alpha|$ parameter presents higher value than 4 (4.6 for M1, 4.8 for M2 and 4.8 for M3) suggesting a diffuse surface [23]. The appearance of the extra peak at $q_S = q_M = 0{,}628\ nm^{-1}$ correlates to distance of 10 nm. This peak is consistent with an orthorhombic crystal structure observed in similar systems – a lecithin-stabilized tetracosane lipid nanoparticle system [29], and a phospholipid stabilizer layer at the solid-liquid interface of dispersed triglyceride nanocrystals [30]. Nevertheless, in order to confirm this interpretation, WAXS (wide angle X-ray scattering) measurements and data simulations are necessary.

The idea to use small angle neutrons scattering (SANS) is to investigate the effects of Dox on the structure changes of the SLN made of soybean oil and Mygliol 812 in a different (large, as mention before) q range as a complementary technique to small angle scattering (SAXS). As described above, it was possible to describe the quality of the surface of the nanoparticle using the scattering intensity $I(q)$ for a q range scale 0.9–1 nm. For the SANS measurements (shows in the Figs. 1 and 2), the exponent present in the scattering intensity $I(q) \sim q^{-\beta}$ reveals that the microscopic structure in the range of 1–100 nm can be interpreted as strongly polydisperse nonfractal objects [34]. As displayed in the Fig. 2, the exponent coefficient $|\beta|$ of both systems tends to 4, which can be explained by the smooth surface of the aggregates in the solution. Also, it can be clearly observed that when the concentration of the Dox in the system is increased (Fig. 2(b) and (d)), both systems reach an exponent coefficient $|\beta|$ of 4. This is an indication that the increasing of the Dox concentration causes more ordering in both systems (S and M). For both systems, S and M, in the absence of Dox, the surfaces are relatively more diffuse resulting in a high fluctuation in the SANS signal. However, when we compare the plain carriers (S0 and M0), we noted that the surface fractal structure of the aggregates for the S0 is more pronounced than the M0. One hypothesis for this difference could be related to carbon-carbon bonds of soybean oil containing 86% of unsaturated fatty acid in its composition and Mygliol 812 which has 99% of saturated fatty acid. Further measurements using other techniques (like transmission electron microscopy (TEM)) need to be performed to confirm these results.

Fig. 3 shows a SANS temperature dependence study of the 6 formulations used in this study for 25 (storage temperature), 37 (body temperature) and 40 °C. It is possible to observe a peak at $q = 1.4\ nm^{-1}$ for systems with Dox (S1, S2, S3, M1, M2, M3), and also for a M0 plain carrier. In the case of soybean (S0) plain carrier, no peak is observed (Fig. 3(a)). The presence of this peak, indicates a periodic structure of 4.5 nm. This spacing can be associated with the thickness of the lamellae, as observed in similar systems as nanostructures of complexes formed between the redox-active lipid bis(n-ferrocenylundecyl) dimethylammonium bromide (BFDMA) and DNA [31,32]. Observe that Dox induces more order in the systems, being more pronounced in the soybean (S) oil SLN systems than in the Mygliol (M) SLN system. The absence of the peak in S0, can be related to the fact of soybean oil contains 86% of unsaturated fatty acid in its composition and consequently the lamellae structure is disordered, showing no peak in the SANS data. This observation corroborates with the decreasing of fluctuation in the SANS data when Dox concentration increases, inducing the SANS curves to flatten out to $|\beta| = 4$ as display in the Fig. 2. However further measurements, like

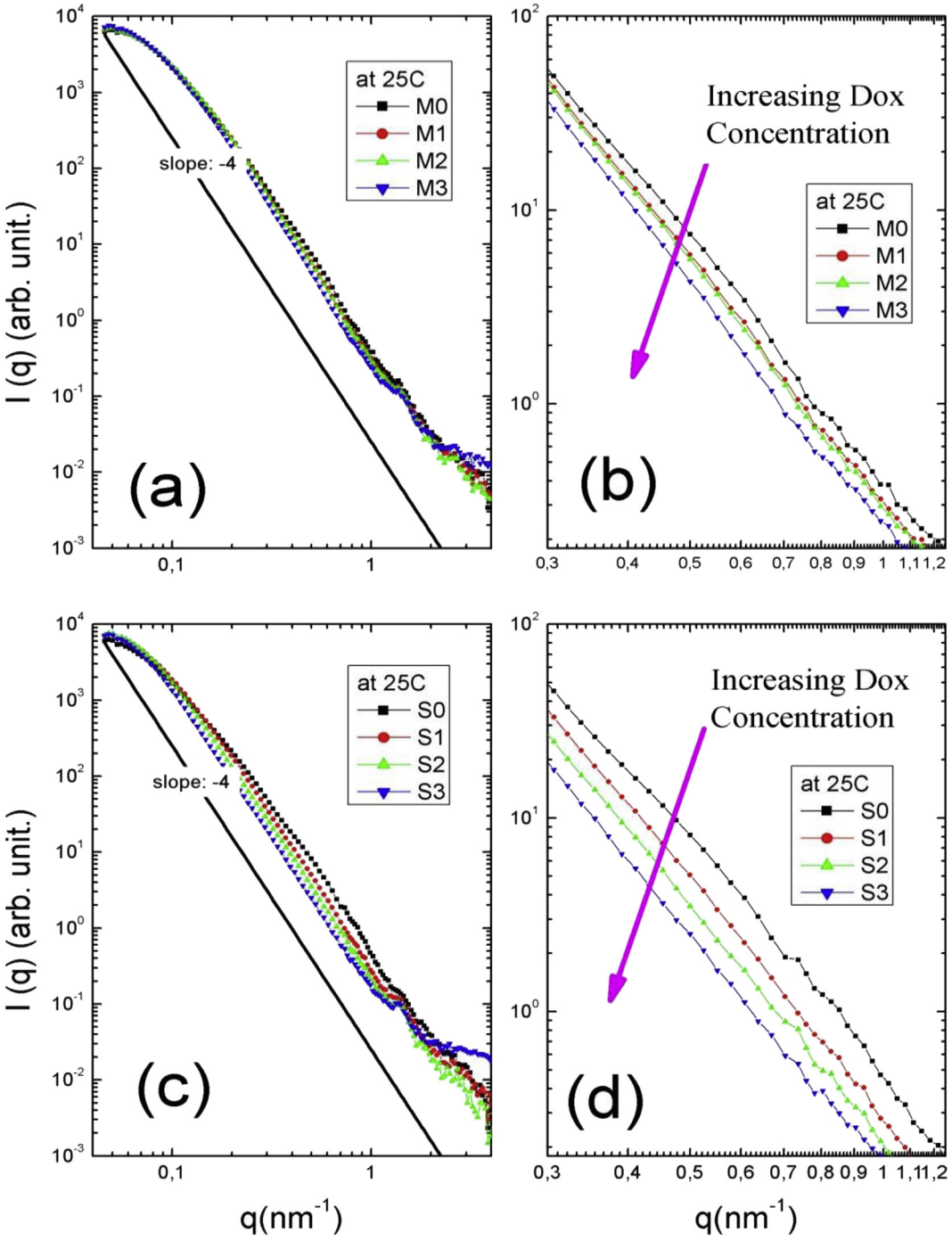

Fig. 2. SANS data comparison for (a,b) Mygliol 812 SLN, and (c,d) Soybean oil SLN, for different Dox concentrations. Observe that the effect of the Doxconcentration in the S(SLN) systems is more pronounced than the M(SLN) system. ((d) and (b), respectively).

X-day diffraction and pair distribution function (PDF) analysis need to be performed in order to confirm these results.

As shown in Fig. 3, Dox causes increased ordering in the mygliol (M) and soy bean (S) systems. This is evident not just by the appearance of the peak at 1.4 nm^{-1} but also because the SANS curves decay flattens out to q^{-4} power law slope as the concentration of Dox increases (decreasing the SLD-Scattering Length Density fluctuations). The closer it is to q^{-4} slope the smoother the surfaces and sharper the interfaces. Without Dox, both systems present relatively diffuse surfaces, with deviations from the q^{-4} behaviour over a wide range of q. A similar decreasing of SLD fluctuations has been observed in other systems such as, starch [35], where the crystallinity behaviour is more pronounced than the amorphous one.

Furthermore, we emphasize that the SLD fluctuations are also affected by the concentration of the salt in these systems. In our study, we observe a decreasing of the SLD fluctuations when the concentration of a salt (Dox) is increasing, as opposed to systems like chondroitin sulfate (a polysaccharide) [36] and poly(N-isopropylacrylamide) (PNIPAM) (a chain polymer) [37]. These two references show that the increasing of concentration of salts, increases the fluctuation in the SANS curves, and consequently affect the ordering of these systems.

4. Conclusion

The development of alternative drug delivery carriers, with a focus on

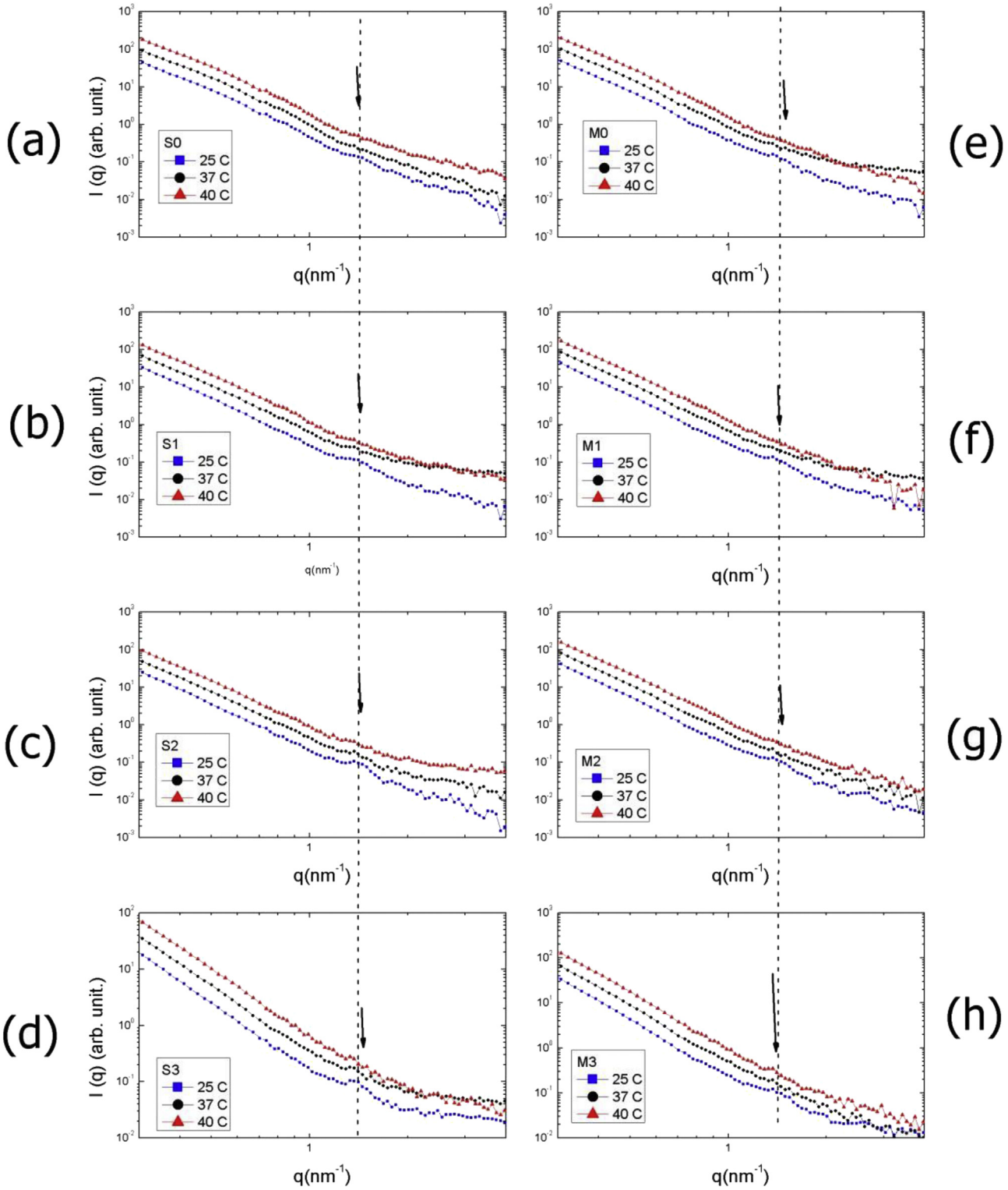

Fig. 3. Temperature dependence of SANS measurements for (a) S0, (b) S1, (c) S2, (d) S3, (e) M0, (f) M1, (g) M2 and (h) M3. Observe the appearance of a small reflection at $q = 1{,}4\ nm^{-1}$ that vanishes at higher temperature (37 and 40 °C). Also, note that this peak is not detected in the S0 system.

cancer treatment with reduced side effects, is a primary goal of recent cancer research. In this study we performed structural analysis of soybean oil or Mygliol 812 solid lipid nanoparticle (SLN) based drug delivery systems using the combination of complementary scattering techniques: small angle neutron scattering (SANS) and small angle X-ray scattering (SAXS). Combining both scattering techniques revealed structural characteristics of these systems, such as the cubic structure and the surface fractality via SAXS measurement, and also observe a strongly polydisperse nonfractal objects that varies with the concentration of the Dox in these systems (via SANS measurement) in a large q range, as a complementarily technique to SAXS data. Indications of an unusual orthorhombic structure (observed via SAXS) and the presence of an extra peak that may indicate the thickness of the lamellae (VSANS), as well as the behaviour of the systems as a function of temperature, still need to be

confirmed with other techniques (like WAXS and PDF analysis). Moreover, in order to obtain a more accurate model for these SLN systems, further analysis also needs to be performed combining SANS and SAXSdata of the SLN systems for soybean oil and Mygliol 812.

Acknowledgment

We would like to thank HZB for the allocation of neutron beamtime.

References

[1] R.L. Siegel, K.D. Miller, A. Jemal, Cancer statistics, CA Canc. J. Clin. 65 (2015) 5–29, https://doi.org/10.3322/caac.21254.
[2] R.L. Siegel, K.D. Miller, A. Jemal, Cancer statistics, CA Canc. J. Clin. 65 (2017) 5–29, https://doi.org/10.3322/caac.21387.
[3] A. Coates, S. Abraham, S.B. Kaye, T. Sowerbutts, C. Frewin, R.M. Fox, M.H. Tattersall, On the receiving end–patient perception of the side-effects of cancer chemotherapy, Eur. J. Canc. Clin. Oncol. 19 (1983) 203–208.
[4] R.R. Love, H. Leventhal, D.V. Easterling, D.R. Nerenz, Side effects and emotional distress during cancer chemotherapy, Cancer 63 (1989) 604–612.
[5] V. Weissig, T.K. Pettinger, N. Murdock, Nanopharmaceuticals (part 1): products on the market, Int. J. Nanomed. 9 (2014) 4357–4373, https://doi.org/10.2147/IJN.S46900.
[6] V. Weissig, D. Guzman-Villanueva, Nanopharmaceuticals (part 2): products in the pipeline, Int. J. Nanomed. 10 (2015) 1245–1257, https://doi.org/10.2147/IJN.S65526.
[7] C. Carvalho, R.X. Sanots, S. Cardoso, S. Correia, P.J. Oliveira, W.S. Sanots, P.I. Moreira, Doxorubicin: the good, the bad and the ugly effect, Curr. Med. Chem. 16 (25) (2009) 3267–3285.
[8] O. Tacar, P. Sriamornsak, C.R. Dass, Doxorubicin: an update on anticancer molecular action, toxicity and novel drug delivery systems, J. Pharm. Pharmacol. 65 (2012) 157–170, https://doi.org/10.1111/j.2042-7158.2012.01567.x.
[9] C.F. Thorn, C. Oshiro, S. Marsh, T. Hernandez-Boussard, H. McLeod, T.E. Klein, R.B. Altman, Doxorubicin pathways:pharmacodynamics and adverse effects, Pharmacogen. Genom. 21 (7) (2011) 440–446, https://doi.org/10.1097/FPC.0b013e32833ffb56.
[10] G. Minotti, P. Menna, E. Salvatorelli, G. Cairo, L. Gianni, Anthracyclines: molecular advances and pharmacologic developments in antitumor activity and cardiotoxicity, Pharmacol. Rev. 56 (2004) 185–229, https://doi.org/10.1124/pr.56.2.6.
[11] C. Palmieri, V. Misra, A. Januszewski, H. Yosef, R. Ashford, I. Keary, N. Davidson, Multicenter experience of nonpegylated liposomal Doxorubicin use in the management of metastatic breast cancer, Clin. Breast Canc. 14 (2014) 85–93, https://doi.org/10.1016/j.clbc.2013.10.011.
[12] M. Fiegl, B. Mlineritsch, M. Hubalek, R. Bartsch, U. Pluschnig, G.G. Steger, Single-agent pegylated liposomal Doxorubicin (PLD) in the treatment of metastatic breast cancer: results of an Austrian observational trial, BMC Canc. 11 (373) (2011), https://doi.org/10.1186/1471-2407-11-373.
[13] K.M. Rau, Y.C. Lin, Y.Y. Chen, J.S. Chen, K.D. Lee, C.H. Wang, H.K. Chang, Pegylated liposomal Doxorubicin (Lipo-Dox®) combined with cyclophosphamide and 5-fluorouracil is effective and safe as salvage chemotherapy in taxane-treated metastatic breast cancer: an open-label, multi-center, non-comparative phase II study, BMC Canc. 15 (423) (2015), https://doi.org/10.1186/s12885-015-1433-4.
[14] Y. Ichikawa, M. Ghanefar, M. Bayeva, R. Wu, A. Khechaduri, S.V. Naga Prasad, R.K. Mutharasan, T.J. Naik, H. Ardehali, Cardiotoxicity of Doxorubicin is mediated through mitochondrial iron accumulation, J. Clin. Invest. 124 (2014) 617–630, https://doi.org/10.1172/JCI72931. Epub 2014 Jan 2.
[15] G. Minotti, P. Menna, E. Salvatorelli, G. Cairo, L. Gianni, Anthracyclines: molecular advances and pharmacologic developments in antitumor activity and cardiotoxicity, Pharmacol. Rev. 56 (2004) 185–229.
[16] S.N. Hilmer, V.C. Coqqer, M. Muller, D.G. le Couteur, The hepatic pharmacokinetics of doxorubicin and liposomal doxorubicin, Drug Metabol. Dispos. 32 (8) (2004) 794–799, https://doi.org/10.1124/dmd.32.8.794.
[17] M.E. O'Brien, N. Wigler, M. Inbar, R. Rosso, E. Grischke, A. Santoro, R. Catane, D.G. Kieback, P. Tomczak, S.P. Ackland, F. Orlandi, L. Mellars, L. Alland, C. Tendler, Reduced cardiotoxicity and comparable efficacy in a phase III trial of pegylated liposomal Doxorubicin HCl (CAELYX/Doxil) versus conventional Doxorubicin for first-line treatment of metastatic breast cancer, Ann. Oncol. 15 (2004) 440–449.
[18] FDA approval of generic version of cancer drug Doxil is expected to help resolve shortage. [http://www.webcitation.org/6Yz2BdWO5] Cached on 6/2/2015, 10:52: 31.
[19] D. Lorusso, A. Di Stefano, V. Carone, A. Fagotti, S. Pisconti, G. Scambia, Pegylated liposomal Doxorubicin-related palmar-plantar erythrodysesthesia ('hand-foot' syndrome), Ann. Oncol. 18 (2007) 1159–1164, https://doi.org/10.1093/annonc/mdl477.
[20] K.P. Farr, A. Safwat, Palmar-plantar erythrodysesthesia associated with chemotherapy and its treatment, Case Rep. Oncol. 4 (2011) 229–235, https://doi.org/10.1159/000327767.
[21] C. Carbone, A. Leonardi, S. Cupri, G. Puglisi, R. Pignatello, Pharmaceutical and biomedical applications of lipid-based nanocarriers, Pharm. Pat. Anal. 3 (2014) 199–215, https://doi.org/10.4155/ppa.13.79.
[22] R.H. Muller, K. Mader, S. Gohla, Solid lipid nanoparticles (SLN) for controlled drug delivery – a review fo the state of art, Eur. J. Pharm. Biopharm. 50 (1) (2000) 161–177, https://doi.org/10.1016/S0939-6411(00)00087-4.
[23] C. Schmidt, F. Yokaichiya, N. Doganguzel, M.K.K.D. Franco, L.P. Cavalcanti, M.A. Brown, M.I. Alkschbirs, D.R. de Araujo, M. Kumpugdee-Vollrath, J. Storsberg, An abraded surface of doxorubicin-loaded surfactant-containing drug delivery systems effectively reduces the survival of carcinoma cells, Biomedicines 4 (2016) 22,, https://doi.org/10.3390/biomedicines4030022.
[24] A. Chinsriwongkul, P. Chareanputtakhun, T. Ngawhirunpat, T. Rojanarata, W. Sila-on, U. Ruktanonchai, Opanasopit. Nanostructured lipid carriers (NLC) for parenteral delivery of an anticancer drug, AAPS PharmSciTech 13 (2012) 150–158, https://doi.org/10.1208/s12249-011-9733-8.
[25] K. Vogtt, M. Siebenburger, D. Clemens, C. Rabe, P. Lindner, M. Russina, M. Fromme, F. Mezei, M. Ballauff, A new time-of-flight small-angle scattering instrument at the Helmhotz-Zentrum Berlin: V16/VSANS, J. Appl. Crystallogr. 47 (2014) 237–244, https://doi.org/10.1107/S1600576713030227.
[26] L.P. Cavalcanti, I.L. Torriani, T.S. Plivelic, C.L.P. Oliveira, G. Kellermann, R. Neuenschwander, Two new sealed sample cells for small angle x-ray scattering from macromolecules in solution and complex fluids using synchrotron radiation, Rev Sci. Instr. 75 (2004) 4541–4546, https://doi.org/10.1063/1.1804956.
[27] P. Georgiades, E. di Cola, R.K. Heenan, P.D.A. Pudney, D.J. Thornton, T.A. Waigh, A combined small-angle X-ray and neutron scattering study of the structure of purified soluble gastrointestinal mucins, Biopolymers 101 (2014) 1154–1164, https://doi.org/10.1002/bip.22523.
[28] E.A. Odo, D.T. Britton, G.G. Gonfa, M. Harting, SAXS study of silicon nanocomposites, Int. J. Comp. Mat. 5 (2015) 65–70, https://doi.org/10.5923/j.cmaterials.20150503.03.
[29] M. Schmiele, S. Busch, H. Morhenn, T. Schindler, T. Schmutzler, R. Schweins, P. Lindner, P. Boesecke, M. Westemann, F. Steiniger, S.S. Funari, T. Unruh, Stuctural characterization of lecithin-stabilized tetracosane lipid nanoparticle. Part II: suspension, J. Phys. Chem. 120 (24) (2016) 5513–5526, https://doi.org/10.1021/acs.jpcb.6b02520.
[30] M. Schmiele, T. Schindler, T. Unruh, S. Busch, H. Morhenn, M. Westermann, F. Steiniger, A. Radulescu, P. Lindner, R. Schweins, P. Boesecke, Structural characterization of the phospholipid stabilizer layer at the solid-liquid interface of dispersed triglyceride nanocrystals with small-angle x-ray and neutron scattering, Phys. Rev. E 87 (2013), 062316, https://doi.org/10.1103/PhysRevE.87.062316.
[31] C.L. Pizzey, C.M. Jeveli, M.E. Hays, D.M. Lynn, N.L. Abbott, Y. Kondo, S. Golan, Y. Talmon, Characterization of the nanostructure of complexes formed by a redox-active cationic lipid and DNA, J. Phys. Chem. B. 112 (18) (2008) 5849–5857, https://doi.org/10.1021/jp7103903.
[32] S. Zhao, X. Yang, V.M. Garamus, U.A. Handge, L. Bérengère, L. Zhao, G. Salamon, R. Willumeit, A. Zou, S. Fan, Mixture of nonionic/ionic surfactants for the formulation of nanostructure lipid carriers: effects on physical properties, Langmuir 30 (2014) 6920–6928, https://doi.org/10.1021/la501141m.
[33] K. Brandenburg, W. Richter, M.H. Koch, H.W. Meyer, U. Seydel, Characterization of the nonlamellar cubic and HII structure of lipid a from Salmonella EntericaSerovar Minnesota by X-ray diffraction and Freeze-fracture electron microscopy, Chem. Phys. Lipid 91 (1998) 53–69, https://doi.org/10.1016/S0009-3084(97)00093-5.
[34] Y. Chen, X. Yang, L. Zhao, L. Almásy, V. Garamus, R. Willumeit, A. Zou, Preparation and Characterization of a nanostructure lipid carrier for poorly soluble drug, Colloids Surf. A: Physicochem. Eng. Aspects 455 (2014) 36–43, https://doi.org/10.1016/j.colsurfa.2014.04.032.
[35] Z. Li, X. Kong, X. Zhou, K. Zhong, S. Zhou, X. Liu, Characterization of multi-scale structure and thermal properties of Indica rice starch with different amylose contents, RSC Adv. 6 (2016) 107491–107497, https://doi.org/10.1039/c6ra17922c.
[36] F. Horkay, P.J. Basser, A.M. Hecht, E. Geissle, Chondroitin sulfate in solution: effects of mono- and divalent salts, Macromolecules 45 (2012) 2882–2890, https://doi.org/10.1021/ma202693s.
[37] D. Jia, M. Muthukumar, H. Cheng, C.C. Han, B. Hammouda, Concentration fluctuations near lower critical solution temperature in ternary aqueous solutions, Macromolecules 50 (2017) 7291–7298, https://doi.org/10.1021/acs.macromol.7b01502.